



HAL
open science

Origins of large light induced voltage in magnetic tunnel junctions grown on semiconductor substrates

Y. Xu, W. Lin, S. Petit-Watelot, Michel Hehn, Hervé Rinnert, Y. Lu, F. Montaigne, D. Lacour, Stéphane Andrieu, S. Mangin

► **To cite this version:**

Y. Xu, W. Lin, S. Petit-Watelot, Michel Hehn, Hervé Rinnert, et al.. Origins of large light induced voltage in magnetic tunnel junctions grown on semiconductor substrates. *Journal of Applied Physics*, 2016, 119, pp.23907 - 23907. 10.1063/1.4939966 . hal-01686955

HAL Id: hal-01686955

<https://hal.univ-lorraine.fr/hal-01686955v1>



Submitted on 2 Aug 2024

HAL is a multi-disciplinary open access archive for the deposit and dissemination of scientific research documents, whether they are published or not. The documents may come from teaching and research institutions in France or abroad, or from public or private research centers.

L'archive ouverte pluridisciplinaire **HAL**, est destinée au dépôt et à la diffusion de documents scientifiques de niveau recherche, publiés ou non, émanant des établissements d'enseignement et de recherche français ou étrangers, des laboratoires publics ou privés.

RESEARCH ARTICLE | JANUARY 14 2016

Origins of large light induced voltage in magnetic tunnel junctions grown on semiconductor substrates






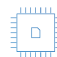
Y. Xu; W. Lin; S. Petit-Watelot; M. Hehn; H. Rinnert; Y. Lu; F. Montaigne ; D. Lacour; S. Andrieu; S. Mangin 

 Check for updates

J. Appl. Phys. 119, 023907 (2016)


<https://doi.org/10.1063/1.4939966>



 Nanotechnology & Materials Science  Optics & Photonics  Impedance Analysis  Scanning Probe Microscopy  Sensors  Failure Analysis & Semiconductors

Unlock the Full Spectrum.
From DC to 8.5 GHz.
Your Application. Measured.

[Find out more](#)



Origins of large light induced voltage in magnetic tunnel junctions grown on semiconductor substrates

Y. Xu, W. Lin, S. Petit-Watelot, M. Hehn, H. Rinnert, Y. Lu, F. Montaigne, D. Lacour, S. Andrieu, and S. Mangin^{a)}

Institut Jean Lamour, UMR CNRS 7198, Université de Lorraine- BP 70239, F-54506 Vandoeuvre-lès-Nancy Cedex, France

(Received 14 August 2015; accepted 5 January 2016; published online 14 January 2016)

Recently, the study of interactions between electron spins and heat currents has given rise to the field of “Spin Caloritronics”. Experimental studies of these interactions have shown a possibility to combine the use of heat and light to power magnetic tunnel junction (MTJ) devices. Here we present a careful study of an MTJ device on Si substrate that can be powered entirely by light. We analyze the influence of the material properties, device geometry, and laser characteristics on the electric response of the sample. We demonstrate that by engineering the MTJ and its electrical contact, a large photovoltage reaching 100 mV can be generated. This voltage originates from the Si substrate and depends on the MTJ magnetic configuration. Finally, we discuss the origin of the photo-voltage in terms of Seebeck and photovoltaic effects. © 2016 AIP Publishing LLC.

[<http://dx.doi.org/10.1063/1.4939966>]

I. INTRODUCTION

Devices built from thin ferromagnetic and non-magnetic layers such as MTJs^{1–3} opened a new field called spintronics.^{4,5} MTJs are now used for a wide variety of applications, such as Magnetic Random Access Memories (MRAM),^{6,7} Magnetic Logic,^{8,9} Magnetic Sensors,¹⁰ and, more recently, Memristors.¹¹ MTJs are made of an insulating barrier between two layers; a free layer and a fixed layer. The free magnetic layer has a magnetization orientation that can easily follow an external field, while the fixed magnetic layer is insensitive to small applied field on the magnitude of the operation of the device. These devices are based on the principle that two different magnetic states (P and AP states corresponding, respectively, to a Parallel or an Anti-Parallel orientation of the two magnetic layers) generate two different resistances (R_P and R_{AP}). The devices are useful as Tunnel Magneto-Resistance ($TMR = (R_{AP} - R_P)/R_P$) can now reach more than 600% in CoFeB/MgO/CoFeB MTJ devices at room temperature.¹² In MRAM devices, the information is read by measuring the resistance via an applied current, while the information is written by a separate current-driven external magnetic field. Due to the inefficiencies inherent in generating these external fields, many efforts are made to manipulate the magnetization by other means. In order to increase device speed and decrease energy consumption, a new method of magnetization manipulation is needed. It has already been demonstrated that an injected polarized current can very efficiently switch the magnetization of a free layer thanks to the Spin Transfer Torque (STT) effect.^{13,14} This has led to the concept of STT-MRAM.¹⁵ Other effects like electric field^{16,17} and strain have also been investigated.¹⁸ More recently, optical manipulation of magnetic materials compatible with spintronic devices has been

demonstrated by the use of 100 fs polarized laser pulses.^{19–21} This possibility of optically manipulated magnetization could soon be used in the magnetorecording industry.²¹ If light can be used to change magnetization orientation and thus write information, it is now interesting to know if light can also be used to read the stored information without any current injection. Recently it has also been shown that spin injection is possible with unpolarized light by means of spin solar cell and spin photodiode effect.^{22,23} This offers an exciting possibility of both optical manipulation and reading of the information in MTJ devices.

In this paper we demonstrate that by engineering an MTJ and its electrical contact, a large photovoltage reaching 100 mV can be generated. This voltage originates from the Si substrate and depends on the MTJ magnetic configuration. First, the baseline behavior of the MTJ device is characterized by measuring its conventional tunneling magnetoresistance (TMR), as an external electric source is powering the device. Then we measured the generated voltage across the MTJs in the absence of an external electrical power source but under illuminated power. Three measurements of illumination have been done: (1) as a continuous laser is illuminating the device, which will be referred to as DC measurement, (2) as the laser intensity is modulated at a given frequency while the voltage is measured synchronously, which will be referred to as AC measurement, and (3) as a function of time after a single light pulse (typically 20 ns). The effect of light on this MTJ grown on silicon substrate can then be modelled by a well characterized equivalent electrical circuit. In this general context, light has two effects: it transfers heat that can generate temperature gradients and create thermo-voltages (Seebeck effect) and it generates a photo-current through the photovoltaic effect in the semiconductor substrates. All measurements were performed at room temperature.

The MTJs that were studied are (Si substrate p-low doping (20 k Ω cm)/Ta(5 nm)/Co(10 nm)/IrMn(7.5 nm)/Co(5 nm)/

^{a)}Author to whom correspondence should be addressed. Electronic mail: stephane.mangin@univ-lorraine.fr.

$\text{Al}_2\text{O}_3(2\text{ nm})/\text{Co}(10\text{ nm})/\text{Pt}(5\text{ nm})$). Then two types of device geometries were processed as sketched in Figures 1(c) and 1(d). One called “No Contact” is a “conventional” design where the top lead is insulated from the substrate by a 150 nm SiO_2 thick insulating layer (Fig. 1(c)). The second one is called “Contact” where a direct metallic Ta/Au connection from the top lead to the substrate completes the electrical circuit including the MTJ in parallel with the substrate (Fig. 1(d)). The size of the junction pillar is $20 \times 20\ \mu\text{m}^2$ and in the case of the contact geometry the metallic connection is 760×760 or $20 \times 20\ \mu\text{m}^2$.

II. AC/DC PHOTO-VOLTAGE ON MAGNETIC TUNNEL JUNCTION

Figure 1 and its subfigures show the evolution of the two systems (“Contact” and “No Contact”) under different perturbations. Figures 1(a) and 1(b) show the evolution of the resistance under swept magnetic field. Figures 1(e) and 1(f) show the DC photo-voltage generated when a laser diode is shining at the sample from 5 mm above the tunnel junction.

It is important to first note that the TMR signal (Figs. 1(a) and 1(b)) is not affected by the device geometry (“Contact” or

“No Contact”). In the “Contact” geometry, the resistance of the MTJ in the P and AP states is small compared with the resistance of the parallel branch that includes the substrate and contact resistances. Equivalent circuits are sketched in Figures 1(g) and 1(h). Moreover, the contact resistance between the substrate and metallic contact includes a Schottky barrier (SB) that will be examined later. Consequently, the TMR signal cannot be used as an indication of “Contact” or “No Contact” geometry. When the device is not powered by an electric source but is illuminated by a laser diode from 5 mm above the junction in the “No Contact” geometry, the measured DC voltage does not noticeably change with the magnetic field (Fig. 1(e)). Results of this measurement imply that there is no detectable spin dependent voltage created across the studied MTJ. This result is confirmed if the Si substrate is replaced by an insulating glass substrate. However, in the case of the “Contact” geometry, the DC measured voltage presents a magnetic hysteresis loop comparable with the TMR signal.

By replacing the voltmeter by an ammeter, a DC current can also be measured. Figures 2(c) and 2(d) show the measured current as a function of external field for the “No Contact” sample and “Contact” sample, respectively. The current for “No Contact” sample is negligible and this is in agreement with the voltage measurement presented in Figure 1(e). The current for the “Contact” sample reaches $7.4\ \mu\text{A}$ and is independent of the magnetic configuration. Several studies have shown that hot electrons generated in a semiconductor could give rise to effects such as hot electron spin-valve effect.^{24–27} Note that hot electrons can only travel on short distances (tens of nm),²⁶ which is much smaller than the dimensions of our system (hundreds of μm).

The situation is different when using square wave modulated light. Figures 3(a) and 3(b) present the evolution of the AC voltage as a function of the applied field for both geometries. A significant AC voltage is observed for both “No Contact” and “Contact” geometries, which depends on the magnetic configuration of the MTJ. This is displayed in

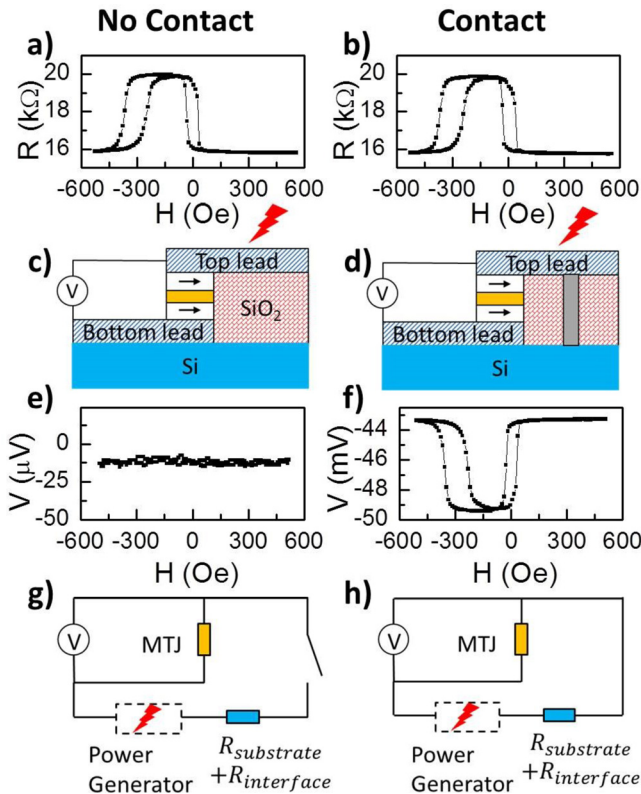


FIG. 1. Presentation of two MTJs of multilayer stack: Ta(5 nm)/Co(10 nm)/IrMn(7.5 nm)/Co(5 nm)/ $\text{Al}_2\text{O}_3(2\text{ nm})/\text{Co}(10\text{ nm})/\text{Pt}(5\text{ nm})$ grown on a Si substrate in “No Contact” (left panel) and “Contact” (right panel) geometries. (a) and (b) Resistance (R) of the devices as a function of the in-plane applied field (H). A DC bias voltage of 10 mV was applied for the resistance measurements. (c) and (d) Schematic of the devices in a DC voltage measurement configuration. (e) and (f) DC voltage (V) measured as a function of the in-plane applied field (H) as sketched in (c) and (d) when the MTJ is illuminated by a laser (power 59 mW). (g) and (h) Schematic of the equivalent circuits that correspond to the two geometries.

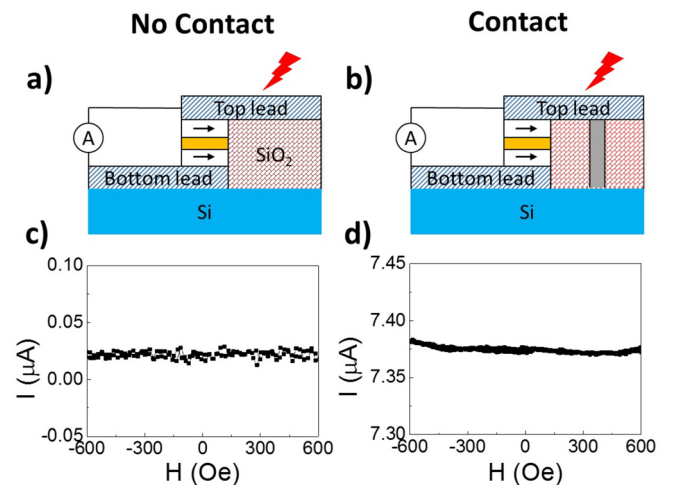


FIG. 2. DC current measurement in “No Contact” (left panel) and “Contact” (right panel) geometries. (a) and (b) Schematic of the devices in the current measurement configuration. DC current is measured when the MTJ is illuminated by a laser (59 mW). (c) and (d) Current (I) as a function of magnetic field (H) for the two geometries.

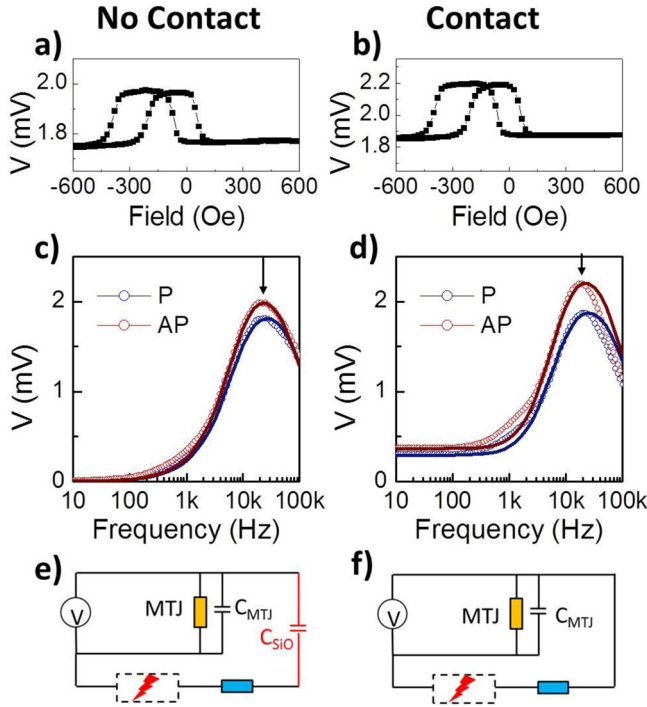


FIG. 3. For each MTJ sample in Figure 1 (“No Contact” (left panel) and “Contact” (right panel)) an oscillating laser pulse of varying frequency was applied and the voltage response measured. (a) and (b) AC voltage (V) as a function of field (H) measured for a laser excitation of 20 kHz, 5.4 mW. (c) and (d) Frequency dependence of the AC voltage (V) for P and AP states. Empty dots correspond to the experimental data and solid lines correspond to the fitting considering an equivalent electrical circuit. (e) and (f) Sketch of the equivalent electrical circuits (a detailed circuit is presented in the following).

Figures 3(a) and 3(b) (the laser diode illuminates the device with a power of 5.4 mW and a frequency of 20 kHz and without an external electric source to the device). The AC voltage evolution with field is again comparable with the TMR signal, leading to a voltage difference between P and AP states equal to 0.2 mV. This AC voltage amplitude between P and AP states is also observed to vary strongly with the modulation frequency of the light as shown in Figures 3(c) and 3(d). When moving toward low frequency, the results are consistent with those shown in Figures 1(e) and 1(f) while in the “No Contact” geometry the voltage no longer depends on the magnetic state.

Those behaviors can be evaluated by starting with an equivalent circuit similar to the one of Figures 1(g) and 1(h) but with the addition of two capacitors (Figs. 3(e) and 3(f)). One capacitor originates from the SiO_2 insulating layer between the top lead and the substrate, and the other from the tunneling barrier inside the MTJ. The experimental data in Figures 3(c) and 3(d) can thus be fitted by adjusting the values of the different resistances and capacitances. An excellent agreement (Figs. 3(c) and 3(d)) is obtained using the full equivalent circuit shown in Figure 4 and considering the following parameters: the resistance of the MTJ (R_{MTJ}), the capacitance of the MTJ (C_{MTJ}), resistance of the substrate (R_{Si}), the capacitance of SiO_2 insulator that separates the top lead and substrate (C_{SiO}), the SB between bottom lead and substrate (SB1), the internal current source of

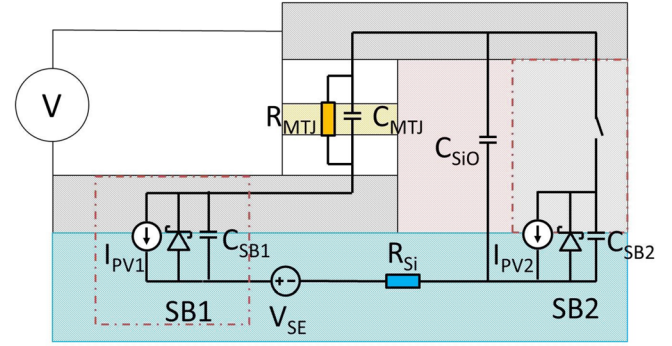


FIG. 4. Schematic of the full equivalent circuit using the following parameters: the resistance of the MTJ (R_{MTJ}), the capacitance of the MTJ (C_{MTJ}), resistance of substrate (R_{Si}), the capacitance of SiO_2 insulator that separates the top lead and substrate (C_{SiO}), the Schottky barrier between bottom lead and substrate (SB1), the internal current source of Schottky barrier under laser (I_{PV}), the voltage source due to Seebeck effect (V_{SE}), and the Schottky barrier in the case of contact geometry (SB2).

Schottky barrier under laser (I_{PV}), the voltage source due to Seebeck effect (V_{SE}), and the Schottky barrier in the case of contact geometry (SB2). The values of those parameters shown in Table I are obtained either from a direct measurement, a simple calculation, or adjusted to be in agreement with values from the literature.

As a preliminary conclusion it is clear that the light interacting with our sample acts as an electric generator. This can be considered without loss of generality as a Norton or Thevenin generator located in the branch formed by the contact and the substrate (Figs. 4 and 6(a)). Several experimental studies reporting the effect of heat on MTJs have been published recently.^{28–31} In Ref. 30 our group has described the large measured voltage in terms of pure Seebeck effect due to a temperature gradient across the tunnel barrier. Since the AC and DC voltages reported here have similar characteristics as in Ref. 30 we believe that the large effect could be the result of an experimental artifact. Indeed, in the following we confirm that a thermo-voltage

TABLE I. Parameters used to simulate the frequency dependence shown in Figure 3. The capacitors of the MTJ and the SiO_2 layer that separates top lead and silicon are given by estimation using parallel-plate model. Resistance of MTJ at P and AP configurations and resistance of silicon are determined by experiments. We have no direct access to the capacitor due to the Schottky barrier, but the values are chosen to be close to the reported values in Refs. 35 and 36. For the sake of simplicity, the Schottky barriers have been treated as simple resistance for AC measurements. As the Si substrate resistance varies with temperature, the value given here corresponds to laser power of 5.4 mW.

		No contact	Contact	Source
Capacitor of MTJ	C_{MTJ}	40 pF	40 pF	Estimated
Resistance of MTJ at AP	$R_{MTJ AP}$	20 k Ω	20 k Ω	Measured
Resistance of MTJ at P	$R_{MTJ P}$	16 k Ω	16 k Ω	Measured
Resistance of substrate	R_{Si}	100 k Ω	100 k Ω	Measured
Capacitor of insulator	C_{SiO}	115 pF	115 pF	Estimated
Capacitor of bottom SB	C_{SB1}	30 pF	30 pF	Ref. 35
Resistance of bottom SB	R_{SB1}	40 k Ω	40 k Ω	Ref. 35
Capacitor of top SB	C_{SB2}	...	30 pF	Ref. 36
Resistance of top SB	R_{SB2}	...	950 k Ω	Ref. 36

exists but we demonstrate that in this system the main contribution comes from the interaction between the light and the substrate. In a context where more and more studies concentrate on electron and spin transport in the presence of temperature gradient and light^{28–33} our measurements underline effects that should be taken into account. Even when a “normal” TMR signal is observed, experimentalists may need to be wary of the presence of an unexpected contact!

Moreover, those results demonstrate the possibility of a light powered MTJ. Indeed such a large photo-voltage obtained on MTJ grown on Si (with a low resistance contact from the top lead to Si) can be used to light-power spintronic applications. The photo-voltage is large enough to enable the determination of the MTJ magnetic states, in both “No Contact” and “Contact” geometries, by using AC light or continuous light, respectively.

III. DISCUSSION ON THE PHYSICAL ORIGIN OF THE PHOTO-VOLTAGE

To study the light interaction with the substrate, the influence of the laser excitation (position of the laser spot, wavelength, and laser power) has been studied on a simplified version of the sample. We observed that the effects responsible for the photo voltages occur when shining light on the substrate or/and at the interface substrate/metal leads. We have studied simplified devices consisting of a Si substrate with two metallic contacts deposited on top (Fig. 5(a)). The $1 \times 1 \text{ mm}^2$ square contacts are made of Ta and are 1.5 mm apart (center to center). In Figure 5(b), the influence of position of the $10 \text{ }\mu\text{m}$ diameter laser spot on the voltage measured between the two contacts is presented. The voltage intensity is the largest when the laser illuminates the substrate close to the leads. As we move the laser spot away from a lead, the intensity decreases. Moreover, it is clear from Figure 5(b) that the signal amplitude is much larger close to the edges than in the middle of the contact. The voltage also changes sign when we move from one lead toward the other lead. One can then conclude that the signal is maximal when the laser shines at a position close to the Si/metal interface.

To improve understanding of the light-matter interaction mechanism, time and wavelength dependences of the photo-voltage were carried out. The voltage was measured in the time range of $0\text{--}200 \text{ }\mu\text{s}$ after a 20 ns laser pulse excitation illuminated the substrate close to one of the leads. Laser wavelength ranged from 400 to 2200 nm . Figures 5(c) and 5(d) show a large intensity peak less than $1 \text{ }\mu\text{s}$ after the laser pulse whereas a broader peak is measured for typical time of $50 \text{ }\mu\text{s}$. Those two peaks behave differently with laser wavelength and the nature of sample holder which suggests that two separated effects coexist in the system.

Focusing on the first peak, we observe that it vanishes when the wavelength is larger than 1100 nm (Fig. 5(c)), corresponding to photon energy lower than 1.12 eV (Si bandgap). From these results we attribute the first peak to a photovoltaic effect. Indeed light with an energy larger than the gap would create electron-hole pairs that would flow through the device. The time scale of the first peak is less than $1 \text{ }\mu\text{s}$, which is consistent with reported values.³⁴

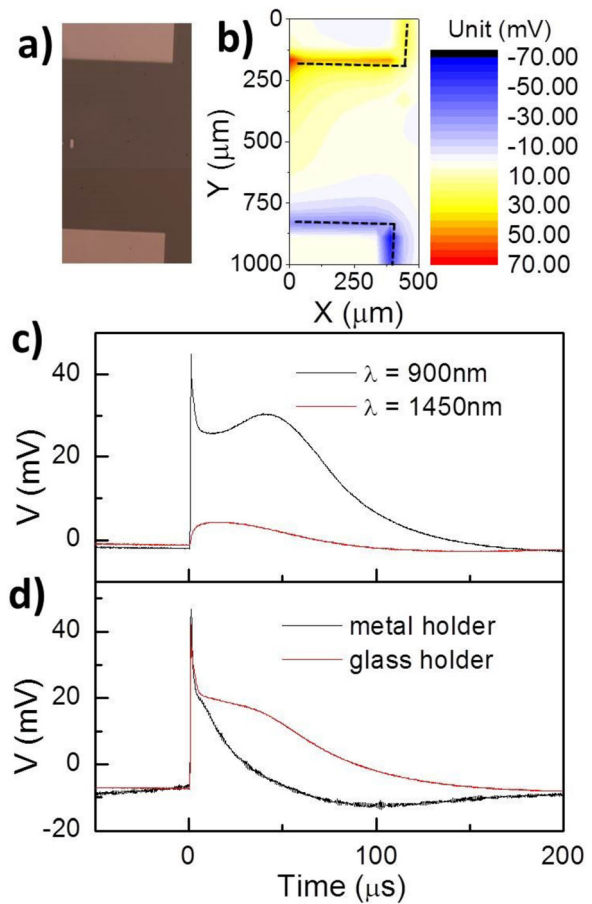


FIG. 5. Measurement on a simplified sample made of two contacts deposited on a Si substrate connected with a voltmeter. (a) Picture of the sample. (b) Evolution of the DC voltage (V) measured by the voltmeter as a function of the laser spot position (X,Y) on the sample. (c) Time resolved signal after a 20 ns laser pulse for 900 nm and 1450 nm wavelengths for the sample on a glass holder. (d) Time resolved signal after a 20 ns laser pulse for a 750 nm wavelength for sample on a metal holder and a glass holder.

The origin of the second peak is different. The photovoltaic effect alone is no longer sufficient as an explanation, and Seebeck effects must be considered. First, peak intensity strongly depends on the nature of the sample holder. In the case of the metal sample holder presented in Figure 5(d), the effect is significantly diminished. As the penetration depth of a 900 nm laser is around $30 \text{ }\mu\text{m}$ in Si, the nature of the holder only influences the boundary conditions of thermal propagation. The glass sample holder can be viewed as a thermal insulator, while the metal sample holder has much higher thermal conductivity. Consequently, the metallic sample holder behaves as a heat sink. This gives credit to the observation that the second peak is linked to a generated temperature gradient. We would attribute the second peak to a Seebeck effect in the Si substrate and/or Si/Ta contact. To evaluate this, we have performed COMSOL simulations to calculate the temperature gradient between the two leads. Assuming that all the laser power is absorbed in Si, a temperature difference reaching a few tens of degrees can be generated during a time scale of tens of microseconds after the pulse. Experimental observations support this model of the behavior. The characteristic of the first peak is independent on the nature of sample holder, in agreement with our conclusions.

The two effects generate a charge accumulation that can flow through the MTJ only if the circuit is closed, which explains the difference between the “Contact” and “No Contact” geometries. In the particular case of a photovoltaic effect, a Schottky barrier is needed to separate electron-hole pair and give rise to a flowing current (avoiding recombination). Note that both effects are expected to decrease as the laser spot is moved away from the contact pad and even change sign when illumination is moved from one contact to the other. If the laser is moved away from the contact, electron-hole pairs will be created farther from the substrate/lead interface, and will be more likely to recombine. Additionally, it is expected that if the laser is moved away from one of the leads, the temperature gradient will also decrease.

In order to test the influence of the substrate on the effect we have grown the same stack on a glass substrate and on GaAs substrate. On the glass substrate no field dependent signal could be detected whereas on a GaAs substrate a strong field dependent voltage similar to the one shown in Figure 1 could be detected. Since glass is an insulator and GaAs is a semiconductor those findings are in agreement with the reported results.

IV. DESCRIPTION OF THE EQUIVALENT ELECTRICAL GENERATOR

From these results we can now describe in more detail the equivalent electrical generator. The Seebeck contribution can be viewed as a voltage source in the Si circuit and the photovoltaic effect can be described as a current source in parallel to each Schottky barrier formed by the contact between the semiconductor substrate and the bottom and top metallic leads (Fig. 6). For the sake of simplicity, the two opposite Schottky diodes can be described as a single effective Schottky diode to the small voltage limit. Moreover from an electrical point of view, it is equivalent to consider the different electrical sources as an effective current source (I_{PV}) in parallel with a single mean Schottky diode as shown in Fig. 6(a). In order to analyze quantitatively the behavior of such generator we performed $I(V)$ curves on a “Contact” MTJ sample for the two magnetic states and for various power intensities as shown in Figures 6(b) and 6(c). In these figures, V is the voltage applied between the two leads (see Fig. 6(a)) and I is the total measured current into the circuit. From Figure 6(a) right, we obtained the following electrical equations:

$$\begin{cases} I = I_S + I_{MTJ} \\ V = V_S + I_S R_{Si}, \end{cases} \quad (1)$$

where $I_S = I_0[\exp(\frac{eV_S}{kT}) - 1] + I_{PV}$. I_0 stands for the dark saturation current,³⁵ I_{PV} the light induced current, and V_S the voltage at the level of the effective source. Figure 6(b) shows $I(V)$ curve measured for the two MTJ magnetic states (AP and P). Here the current I passing through the ammeter (shown in Fig. 6(a)) is measured, while the MTJ is biased with a variable DC voltage (V) and a laser is continuously illuminating the substrate. Note that for zero voltage the current does not depend on the magnetic configuration, whereas

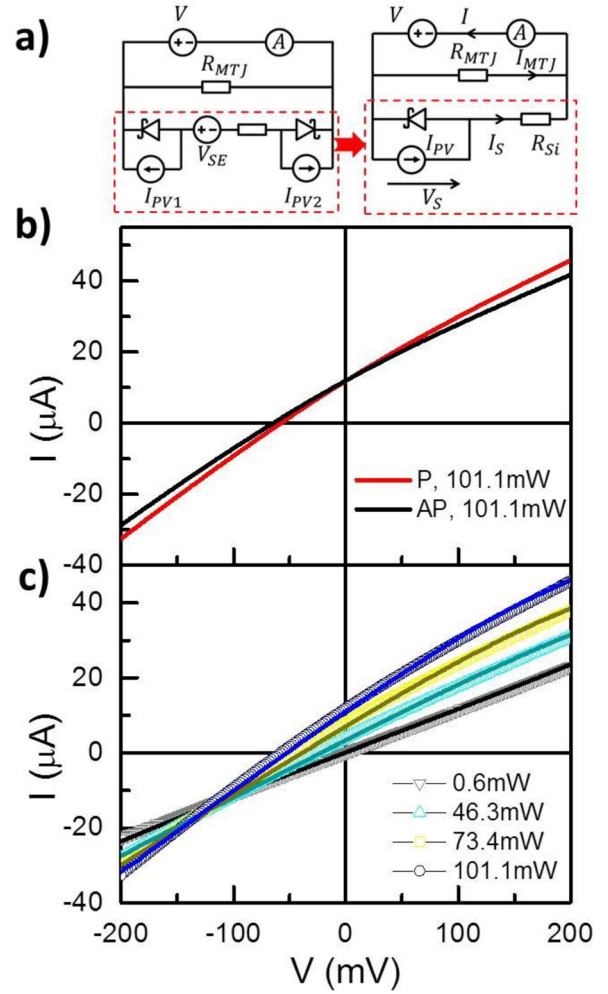


FIG. 6. (a) Sketch of the electric circuit used to model the $I(V)$ curves, in which R_{MTJ} is the resistance of MTJ, R_{Si} the resistance substrate, V_{SE} the Seebeck voltage, and I_{PV1} and I_{PV2} are the photo generated currents of the two SBs, respectively. The two SBs are equivalent to an effective SB (see red dashed boxes), the photocurrent of which is given by I_{PV} . Voltage V is set by an external voltage source, and I the total current of two branches, including the current through MTJ I_{MTJ} and the current through substrate I_S . (b) $I(V)$ curves for P and AP magnetic configuration obtained on the “Contact” geometry device. (c) $I(V)$ for the P magnetic configuration for different laser power. The empty symbols correspond to the experimental data and the solid lines correspond to the fitting.

for zero current the voltage depends on the magnetic configuration (Fig. 1(e)). The curves can be described as the sum of a linear part with an offset and a deviation from the linearity. The linear behavior is essentially due to the Ohmic behavior of the substrate and of the MTJ. The two different slopes for P and AP are due to the two different resistance values of the two states. The offset comes from the equivalent current source due to the laser illumination. The deviation from linearity is due to the effective Schottky diode. In effect, the two Schottky diodes generate an asymmetric electric field which can extract the laser-generated electrons from the silicon. Note that if the two electrode contacts are symmetric and the illumination spot at equal distance from the two contacts no photo-current can be created.

In Figure 6(c) the evolution of the $I(V)$ curves for different light power are presented while the MTJ is kept in the P magnetic state by applying an external field. At zero voltage

TABLE II. Values used for the fitting of I-V curves in Figure 6. The dark saturation current is kept as a constant 1×10^{-7} A. As the laser power increases, the density of excited carriers increases and thus R_{Si} and I_{PV} increase. Values of R_{Si} for different laser power are extracted from the linear part of the IV curves.

Laser power (mW)	R_{Si} (Ω)	I_{PV} (A)
0.6	1×10^5	0.8×10^{-6}
46.3	2.2×10^4	8.7×10^{-6}
73.4	1.2×10^4	1.6×10^{-5}
101.1	8.7×10^3	2.3×10^{-5}

the current increases with the laser power because I_{PV} is directly linked to the laser intensity. The different $I(V)$ curves are perfectly fitted by the set of Equation (1) with the parameters used for the fit in Figure 6(c). The only free parameters are R_{Si} and I_{PV} that depend on the laser power (Table II). We can observe in Figure 6(c) a convergent point for a bias voltage around -100 mV, independent of the laser power. This point depends on the asymmetry between the two diodes described earlier. At this bias point, the electrical field inside the Si substrate becomes symmetric, and consequently the electrons generated by the light can no longer flow in the circuit no matter how much light intensity is used.

From this study the light induced electrical behavior of MTJs on multiple substrates in geometries with or without substrate contacts can be fully described by the equivalent circuit in Figure 4 using the values of different electrical parameters for the samples studied.

V. CONCLUSION

In conclusion, we have demonstrated that the magnetic configuration inside an MTJ can be probed by illuminating spintronic devices without any external current source. A large voltage can be measured using either continuous or pulsed light. The light acts as an additional generator and the system (sample + light) response can be modelled by an equivalent electrical circuit. By growing model systems on various substrates and using continuous and pulsed lasers we propose two different origins for the photo generated voltage. First a photovoltaic effect can be detected in the structures where a semiconductor substrate is used. The effect would rise from the creation of an electron-hole pair which leads to charge propagation through the magnetic tunnel junction if a Schottky barrier is formed between the substrate and the lead. Such a signal is found to vanish once the light's wavelength reaches a critical value (1100 nm for Si) which corresponds to the energy band gap inside the semiconductor. Second, a Seebeck effect could also be detected originating from a temperature gradient between the two parts of the electrical circuit formed by the MTJ, the leads, the substrate, and the insulator. We are able to fully describe the electrical behavior of the devices and we have highlighted the different key parameters that govern the latter.

ACKNOWLEDGMENTS

We would like to thank G. Langaigine for technical assistance with lithography process, and E. E. Fullerton, J.

Sun, and R. Tolley for fruitful discussion. This work was supported by the ANR-NSF Project, ANR-13-IS04-0008-01 "COMAG" by the ANR-Labcom Project LSTNM and The Partner University Fund "Novel Magnetic Materials for Spin Torque Physics" as well as the European Project (OP2M FP7-IOF-2011-298060), The Chinese Government scholarship schemes (CSC) for funding Y.X. PhD, and the Region Lorraine.

- ¹M. Julliere, *Phys. Lett. A* **54**, 225 (1975).
- ²T. Miyazaki and N. Tezuka, *J. Magn. Magn. Mater.* **139**, L231 (1995).
- ³J. S. Moodera, L. R. Kinder, T. M. Wong, and R. Meservey, *Phys. Rev. Lett.* **74**, 3273 (1995).
- ⁴S. A. Wolf, D. D. Awschalom, R. A. Buhrman, J. M. Daughton, S. Von Molnar, M. L. Roukes, A. Y. Chtchelkanova, and D. M. Treger, *Science* **294**, 1488 (2001).
- ⁵A. Fert, J.-M. George, H. Jaffrès, R. Mattana, and P. Seneor, *Europhys. News* **34**, 227 (2003).
- ⁶J. M. Daughton, *J. Appl. Phys.* **81**, 3758 (1997).
- ⁷S. S. P. Parkin, K. P. Roche, M. G. Samant, P. M. Rice, R. B. Beyers, R. E. Scheuerlein, E. J. O'Sullivan, S. L. Brown, J. Bucchigano, D. W. Abraham, Y. Lu, M. Rooks, P. L. Trouilloud, R. A. Wanner, and W. J. Gallagher, *J. Appl. Phys.* **85**, 5828 (1999).
- ⁸W. C. Black, Jr. and B. Das, *J. Appl. Phys.* **87**, 6674 (2000).
- ⁹A. Ney, C. Pampuch, R. Koch, and K. H. Ploog, *Nature* **425**, 485 (2003).
- ¹⁰M. Tondra, J. M. Daughton, D. Wang, R. S. Beech, A. Fink, and J. A. Taylor, *J. Appl. Phys.* **83**, 6688 (1998).
- ¹¹P. Krzysteczko, G. Reiss, and A. Thomas, *Appl. Phys. Lett.* **95**, 112508 (2009).
- ¹²S. Ikeda, J. Hayakawa, Y. Ashizawa, Y. M. Lee, K. Miura, H. Hasegawa, M. Tsunoda, F. Matsukura, and H. Ohno, *Appl. Phys. Lett.* **93**, 082508 (2008).
- ¹³Y. Liu, Z. Zhang, P. P. Freitas, and J. L. Martins, *Appl. Phys. Lett.* **82**, 2871 (2003).
- ¹⁴S. Mangin, Y. Henry, D. Ravelosona, J. A. Katine, and E. E. Fullerton, *Appl. Phys. Lett.* **94**, 012502 (2009).
- ¹⁵Y. Huai, F. Albert, P. Nguyen, M. Pakala, and T. Valet, *Appl. Phys. Lett.* **84**, 3118 (2004).
- ¹⁶T. Nozaki, Y. Shiota, M. Shiraishi, T. Shinjo, and Y. Suzuki, *Appl. Phys. Lett.* **96**, 022506 (2010).
- ¹⁷W.-G. Wang, M. Li, S. Hageman, and C. L. Chien, *Nat. Mater.* **11**, 64 (2012).
- ¹⁸S. S. P. Parkin, C. Kaiser, A. Panchula, P. M. Rice, B. Hughes, M. Samant, and S.-H. Yang, *Nat. Mater.* **3**, 862 (2004).
- ¹⁹C. D. Stanciu, F. Hansteen, A. V. Kimel, A. Kirilyuk, A. Tsukamoto, A. Itoh, and T. Rasing, *Phys. Rev. Lett.* **99**, 047601 (2007).
- ²⁰S. Mangin, M. Gottwald, C.-H. Lambert, D. Steil, V. Uhlir, L. Pang, M. Hehn, S. Alebrand, M. Cinchetti, G. Malinowski, Y. Fainman, M. Aeschlimann, and E. E. Fullerton, *Nat. Mater.* **13**, 286 (2014).
- ²¹C.-H. Lambert, S. Mangin, B. S. D. C. S. Varaprasad, Y. K. Takahashi, M. Hehn, M. Cinchetti, G. Malinowski, K. Hono, Y. Fainman, M. Aeschlimann, and E. E. Fullerton, *Science* **345**, 1337 (2014).
- ²²B. Endres, M. Ciorga, M. Schmid, M. Utz, D. Bougeard, D. Weiss, G. Bayreuther, and C. H. Back, *Nat. Commun.* **4**, 2068 (2013).
- ²³F. Bottegoni, M. Celebrano, M. Bollani, P. Biagioni, G. Isella, F. Ciccacci, and M. Finazzi, *Nat. Mater.* **13**, 790 (2014).
- ²⁴P. H. P. Koller, "Photoinduced transport in magnetic layered structures," Ph. D. thesis, Eindhoven University of Technology, 2004.
- ²⁵I. Appelbaum, D. J. Monsma, K. J. Russell, V. Narayanamurti, and C. M. Marcus, *Appl. Phys. Lett.* **83**, 3737 (2003).
- ²⁶B. Huang and I. Appelbaum, *J. Appl. Phys.* **100**, 034501 (2006).
- ²⁷B. Huang, I. Altfeder, and I. Appelbaum, *Appl. Phys. Lett.* **90**, 052503 (2007).
- ²⁸M. Walter, J. Walowski, V. Zbarsky, M. Münzenberg, M. Schäfers, D. Ebke, G. Reiss, A. Thomas, P. Peretzki, and M. Seibt, *Nat. Mater.* **10**, 742 (2011).
- ²⁹N. Liebing, S. Serrano-Guisan, K. Rott, G. Reiss, J. Langer, B. Ocker, and H. Schumacher, *Phys. Rev. Lett.* **107**, 177201 (2011).
- ³⁰W. Lin, M. Hehn, L. Chaput, B. Negulescu, S. Andrieu, F. Montaigne, and S. Mangin, *Nat. Commun.* **3**, 744 (2012).
- ³¹N. Liebing, S. Serrano-Guisan, P. Krzysteczko, K. Rott, G. Reiss, J. Langer, B. Ocker, and H. W. Schumacher, *Appl. Phys. Lett.* **102**, 242413 (2013).
- ³²W. Jiang, P. Upadhyaya, Y. Fan, J. Zhao, M. Wang, L.-T. Chang, M. Lang, K. L. Wong, M. Lewis, Y.-T. Lin, J. Tang, S. Cherepov, X. Zhou,

- Y. Tserkovnyak, R. N. Schwartz, and K. L. Wang, *Phys. Rev. Lett.* **110**, 177202 (2013).
- ³³A. Boehnke, M. Walter, N. Roschewsky, T. Eggebrecht, V. Drewello, K. Rott, M. Münzenberg, A. Thomas, and G. Reiss, *Rev. Sci. Instrum.* **84**, 063905 (2013).
- ³⁴D. H. Auston, *Appl. Phys. Lett.* **26**, 101 (1975).
- ³⁵Y. S. Ocak, M. F. Genisel, and T. Kılıçoğlu, *Microelectron. Eng.* **87**, 2338 (2010).
- ³⁶H. Çetin, B. Şahin, E. Ayyıldız, and A. Türüt, *Phys. B: Condens. Matter* **364**, 133 (2005).